frontiers in Materials

ORIGINAL RESEARCH
published: 26 January 2022
doi: 10.3389/fmats.2022.827608

Green–Light–Driven Poly(*N*-isopropylacrylamide-acrylamide)/Fe_3O_4 Nanocomposite Hydrogel Actuators

Ying Cao[1,2], *Wenjiao Li*[1], *Fengyu Quan*[1,2]*, *Yanzhi Xia*[1,2] *and Zhong Xiong*[1,2]*

[1]College of Materials Science and Engineering, College of Chemistry and Chemical Engineering, Qingdao University, Qingdao, China, [2]Institute of Marine Biobased Materials, State Key Laboratory of Bio-Fibers and Eco-Textiles, Qingdao University, Qingdao, China

Light-responsive hydrogel actuators show attractive biomedical applications for *in vivo* drug delivery tool, surgical tissue repair operation, and vascular cleaning due to its non-contact, rapid, precise, and remote spatial control of light. Conventional visible–light–responsive hydrogels contain special chemical structure or groups, and the difficulty in synthesis results in that few can be applied to fabricate visible–light–driven hydrogel actuators. In this study, based on photothermal effect, surface-modified Fe_3O_4 nanoparticles were incorporated into poly(*N*-isopropylacrylamide-acrylamide) hydrogel by UV photopolymerization, which revealed excellent green–light–responsive volume change. Under a laser irradiation of 200 mW at 520 nm, the bending angle deformation of hydrogel strips with 2.62 wt% Fe_3O_4 reached 107.8°. Strip-shaped hydrogel actuators could be applied to transport tiny objects. Furthermore, a boomerang-like hydrogel actuator was designed and fabricated to drive floating foam on water. By 12 cycles of continuous laser on–off irradiation to a hydrogel actuator underwater, a circular returning movement of the float was accomplished. The study on driving a float using visible–light–triggered hydrogel actuators provides a new idea for the design of light-driven biomedical devices and soft robots.

Keywords: light-driven, hydrogel actuator, poly(N-isopropylacrylamide), photothermal, Fe_3O_4 nanoparticles

OPEN ACCESS

Edited by:
Yangjun Chen,
Wenzhou Medical University, China

Reviewed by:
Jinhye Bae,
University of California, San Diego, United States
Xuan Shouhu,
University of Science and Technology of China, China

***Correspondence:**
Zhong Xiong
xiongzhong22@163.com
Fengyu Quan
quanfengyu@qdu.edu.cn

Specialty section:
This article was submitted to Biomaterials, a section of the journal Frontiers in Materials

Received: *02 December 2021*
Accepted: *04 January 2022*
Published: *26 January 2022*

Citation:
Cao Y, Li W, Quan F, Xia Y and Xiong Z (2022) Green–Light–Driven Poly(N-isopropylacrylamide-acrylamide)/Fe_3O_4 Nanocomposite Hydrogel Actuators. Front. Mater. 9:827608. doi: 10.3389/fmats.2022.827608

INTRODUCTION

Hydrogels are three-dimensional water-swollen polymeric networks, similar to soft tissues, which exhibit dramatic volume changes in response to various environmental stimuli (Li G. et al., 2020; Jiao et al., 2020; Gao et al., 2020). Due to such stimuli responsiveness, they reveal remarkable potential for wide applications, such as smart sensors (Han S et al., 2020; Chayapol et al., 2021) and actuators (Shang et al., 2019; Zhou et al., 2020; Li M. et al., 2020; Zhao et al., 2021), tissue engineering scaffolds (Mantha et al., 2019; Alfredo et al., 2021), biological separation platforms (Nawaz et al., 2019; Kibungu et al., 2021), controlled drug delivery (Han Z et al., 2020; Sun et al., 2020; Fang et al., 2021), and artificial muscles (Pattavarakorn et al., 2013; Shi et al., 2015). Considerable efforts have been made in the development of high-performance, multifunctional hydrogel actuators with regard to material selection, structural design, and actuation mechanisms owing to its applicability in human

body implantable devices (Yang et al., 2019). For hydrogel actuators, light-driving is a safe approach *in vivo* because of the non-contact, rapid, precise, and remote spatial control of light. Shi et al. reported near-infrared (NIR) light-responsive poly(*N*-isopropylacrylamide)/graphene oxide (PNIPAM/GO) nanocomposite hydrogels with ultrahigh tensibility (Shi et al., 2015). Attributing to the photothermal GO nanosheets and thermoresponsive PNIPAM, hydrogel samples revealed ~90% volume decrease when exposed to NIR light (wavelength: 808 nm). Takashima et al. fabricated reversible supramolecular αCD (cyclodextrin)-azobenzene gels for the *trans*–cis isomerization of azobenzene and large association constant of αCD for *trans*-azobenzene, which achieved reversible deformation under alternating irradiation of ultraviolet (UV) and visible light (Takashima et al., 2012). Chen et al. reported a photo-responsive hydrogel with enhanced photo-efficiency and decoupled process of light activation by incorporating the triphenylmethane leucohydroxide and 2-nitrobenzaldehyde molecules into a polyacrylamide hydrogel (Chen et al., 2020). They demonstrated reprogrammable light patterning of the hydrogel with precisely controlled geometry under UV irradiation at 365 nm. On the whole, numerous studies of light-triggered hydrogel actuators focus the light wavelength on UV and NIR bands, and reports of visible–light–responsive hydrogel actuators are relatively few.

For the hydrogel actuator, visible light driving has unique advantages in comparison with UV and NIR. Generally, short-wavelength UV light may generate small light spots, which is helpful for fine manipulation for actuators, whereas high-energy UV irradiation brings detriment to biological tissues (Xi et al., 2019). Long-wavelength NIR light has higher penetration depth for biological specimens than UV and visible light (Lee et al., 2021), whereas, the ideal light intensity attenuates inversely square with the emission distance and is hard to be spatially controlled due to weak visibility. The merits of visible light at 390–780 nm are intuitive and clear for human eyes, which facilitate precise manipulation of hydrogel actuators *in vivo*. Accardo et al. reported a series of azobenzene boronic acids that reversibly controlled the extent of diol binding *via* photochemical isomerization (Accardo et al., 2020). By tethering this photoswitch to a poly(ethylene glycol) star polymer, they could tune the stiffness of covalent adaptable hydrogels using different wavelengths (450–626 nm) of visible light. Unfortunately, the synthesis of azobenzene boric acid with a special chemical structure is not easy, which limits its application in the hydrogels.

In this study, green–light–driven poly(*N*-isopropylacrylamide-acrylamide)/Fe_3O_4 (P(NIPAM-AM)/Fe_3O_4) nanocomposite hydrogel actuators were fabricated. The design of the material is based on that nano-Fe_3O_4 has good light absorption in the visible region at 520 nm and PNIPAM is a thermoresponsive polymer (Zheng et al., 2020). By converting visible light energy into heat using nano-Fe_3O_4, the shape of the hybrid hydrogel could be adjusted effectively. Furthermore, strip-shaped and boomerang-like hydrogel actuators were fabricated and applied to move tiny objects and drive floating foam under green laser irradiation at 520 nm.

EXPERIMENTAL MATERIALS AND METHODS

Materials

N-Isopropylacrylamide (NIPAM) and acrylamide (AM) were purchased from Shanghai Aladdin Biochemical Technology Co., Ltd. *N*, *N*′-methylenebisacrylamide (BIS) was purchased from Chengdu Kelong Chemicals. Phenylbis(2,4,6-trimethylbenzoyl) phosphine oxide (Omnirad 819) as a photoinitiator was purchased from BASF Corporation. Glycerol, dimethyl sulfoxide (DMSO), and ethanol were purchased from Sinopharm Chemical Reagent Co., Ltd. All chemicals were used without further purification.

Experiment

The synthesis and surface modification of Fe_3O_4 NPs were carried out according to our previous studies (Xiong et al., 2018). By grafting 3-(trimethoxysilyl) propyl methacrylate (MPS) onto Fe_3O_4 NPs, MPS-Fe_3O_4 NPs as a photothermal conversion agent obtained good dispersion in ethanol and DMSO. **Figure 1** reveals the preparation procedure for light-driven P(NIPAM-AM)/Fe_3O_4 nanocomposite hydrogel actuators. Typically, 0.033 g of dried surface-modified Fe_3O_4 NPs was dispersed in a mixed solvent containing 55 μl ethanol and 0.263 ml DMSO by ultrasound. Then, AM (0.080 g) and NIPAM (0.40 g) as monomers, Omnirad 819 (0.010 g) as the UV photoinitiator, BIS (0.0027 g) as the crosslinker, and glycerol (0.40 g) as the thickener were added and dissolved to obtain a black pre-gel solution at 25°C. The pre-gel solution was photopolymerized in a sandwiched glass mold (length: 70 mm, width: 20.5 mm, thickness: 0.2 mm) under the irradiation of a high-voltage mercury lamp (wavelength: 365 nm; power: 500 W) for 5 min. The as-prepared gel was taken out and immersed in water to remove the unpolymerized monomers, DMSO, ethanol, and glycerol to obtain the hydrogel. Finally, P(NIPAM-AM)/Fe_3O_4 hybrid hydrogel was cut into various shapes, such as disc, rectangular with a V-notch, and boomerang (**Supplementary Figures S1, S2**), for various application in this research.

Measurements

The morphology and size of the Fe_3O_4 NPs were analyzed using transmission electron microscopy (TEM, Tecnai G2 F30 S-TWIN, FEI, United States) operated at an accelerating voltage of 300 kV. The SEM images were captured by a field emission scanning electron microscope (Regulus8100, Hitachi, Japan). Before SEM observing, the wet hydrogel samples were frozen at −18°C for 12 h in a refrigerator and then freeze-dried for 24 h. The light absorptions were measured on an UV–Vis spectrophotometer (T9, Beijing Purse General Instrument Co., Ltd.). The temperature of the hydrogel under laser irradiation was monitored by using an infrared thermal imager (Fotric 220s, Shanghai, China). The sample was illuminated under a green laser at 520 nm (maximum power: 1 W, Guangzhou Mingtuo

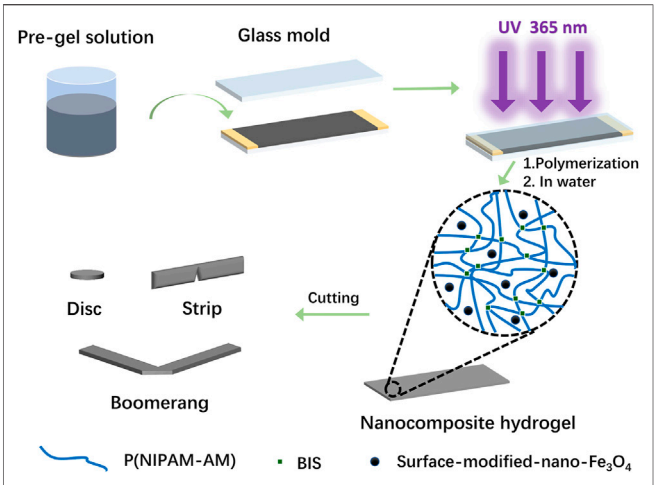

FIGURE 1 | Schematic illustration of the preparation of P (NIPAM-AM)/Fe_3O_4 nanocomposite hydrogel actuators.

Optoelectronics Technology Co., Ltd., Guangdong, China). The laser power can be adjusted by an attenuator.

RESULTS AND DISCUSSION

Characterization of the Hybrid Hydrogel

The morphology of the Fe_3O_4 particles was characterized by TEM. **Figure 2A** reveals the shape of the nanoparticles varying from quasi-sphere to polyhedron with an average size of 8.1 nm. The morphology of the P(NIPAM-AM)/Fe_3O_4 nanocomposite hydrogel was observed by SEM (**Figure 2B**), which shows that the hybrid hydrogel acquires loose and porous structures with pore dimensions ranging from hundreds of nanometers to several micrometers. Aggregation of Fe_3O_4 NPs was observed in dried hydrogel networks (**Figure 2C**). The nanocomposite hydrogel exhibits significant and reversible volume contraction and swelling in water at 80°C and 20°C, respectively (**Figure 3A**). The thermoresponsive shrinkage ratio from 20 to 80°C is as high as 52.86%. Deformation degree (D/D_0) is defined to measure the hydrogel deformation at different temperatures, of which D_0 corresponds to the initial diameter of the hydrogel disc in water at 0°C (ice water mixture) and D corresponds to the diameter of the hydrogel at a specific temperature. After 20 shrink-swelling cycles, the change of D/D_0 reveals good repeatability (**Supplementary Figure S4**). **Figure 3B** shows deformation degrees of P (NIPAM-AM) hydrogels with various Fe_3O_4 contents as a function of temperature. Four deformation degree–temperature curves of P (NIPAM-AM) hydrogels with 0, 1.21, 2.62, and 3.99 wt% of Fe_3O_4 NPs revealed no obvious difference, indicating that nano-Fe_3O_4 content does not affect the thermal-responsive deformation of the hydrogel. For all four hydrogels, volume phase transitions occur in the temperature range of 30~60°C.

As a photothermal conversion agent, surface-modified-Fe_3O_4 NPs were well-dispersed in DMSO, and the UV–Vis absorbance spectrum of the nano-Fe_3O_4/DMSO mixed solution ranging from 300 to 800 nm was measured (**Figure 3C**). Spectrum result indicates that surface-modified Fe_3O_4 NPs have good light absorption at 520 nm, which is lower than that at 300 nm and higher than that at 800 nm. In order to measure the photothermal deformation, the hybrid hydrogel was cut into a rectangular strip (size: 15.5 mm × 1.4 mm × 0.25 mm) with a V-notch in the middle (**Figure 3D**, **Supplementary Figure S1**). In the initial state, the hydrogel strip was immersed in water at 20°C, which exhibited a straight state. When a laser beam (wavelength: 520 nm, power: 200 mW) was focused in the middle of the hydrogel strip above the incision, the hydrogel bended due to volume shrinkage caused by the photothermal effect at the laser focus (**Figure 3D**). The angle between the bending and initial state of the hydrogel is defined as the bending angle θ. The influence of Fe_3O_4 content and laser power on θ of the hydrogel was studied as shown in **Figure 3E**. In general, a high Fe_3O_4 content induces a large θ under the same laser power of 200 mW, which implies that Fe_3O_4 NPs in hydrogels can effectively raise the light absorption and increase the photothermal effect. A large laser power led to a large θ of the nanocomposite hydrogel with same Fe_3O_4 content of 2.62 wt%. The bending angle of the hydrogel with 2.62 wt% Fe_3O_4 NPs reached 107.8° at 200 mW. By turning the laser on or off, the bending behavior can be adjusted reversibly (**Figure 3F**).

The light-driven deformation of the hybrid hydrogel is explained as follows. PNIPAM is one of the well-known thermally responsive polymers, usually characterized by amide and isopropyl groups in the monomer structure, which has a lower critical solution temperature (LCST, ~32°C) in water (Tang et al., 2020). PNIPAM-based hydrogel exhibits a reversible volume change near the LCST. When the laser beam is focused on the hydrogel sample, light energy is absorbed and turned to heat, which induces an increase in temperature. With the increase of temperature higher than LCST, the hydrogen bonds between the hydrophilic amide groups and the water molecules are weakened, and the hydrophobic interactions among the isopropyl groups become strong. In this state, PNIPAM polymer chains are dehydrated and aggregate into a tightly packed conformation, inducing the hydrogel to shrink and exclude water (Yin et al., 2021, **Figure 3A**). On the other hand, when the laser is off, the hydrogel temperature decreases gradually. When the temperature is below the LCST, the hydrogen bonds in the hydrogel counteract the hydrophobic interactions. The PNIPAM polymer chain reveals a flexible and extended conformation in aqueous solution, inducing the hydrogel to a hydrophilic state and swell by absorbing water. Generally, a high Fe_3O_4 content and a high laser power induce a large change of hydrogel temperature and hydrogel deformation.

Light-Driven Transportation

Utilizing the bending deformation of the hybrid hydrogel, transportation of tiny objects can be achieved. As shown in **Figure 4A**, a hydrogel strip actuator with a V-notch was fixed to an aluminum clamper in water, and a small cucumber

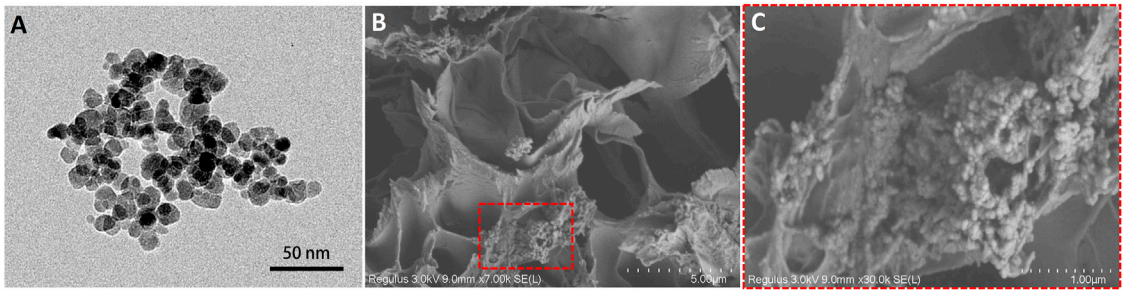

FIGURE 2 | (A) TEM image of surface-modified-Fe_3O_4 NPs. **(B)** SEM image of P (NIPAM-AM)/Fe_3O_4 nanocomposite hydrogel. **(C)** Magnified SEM image of nano-Fe_3O_4 aggregation.

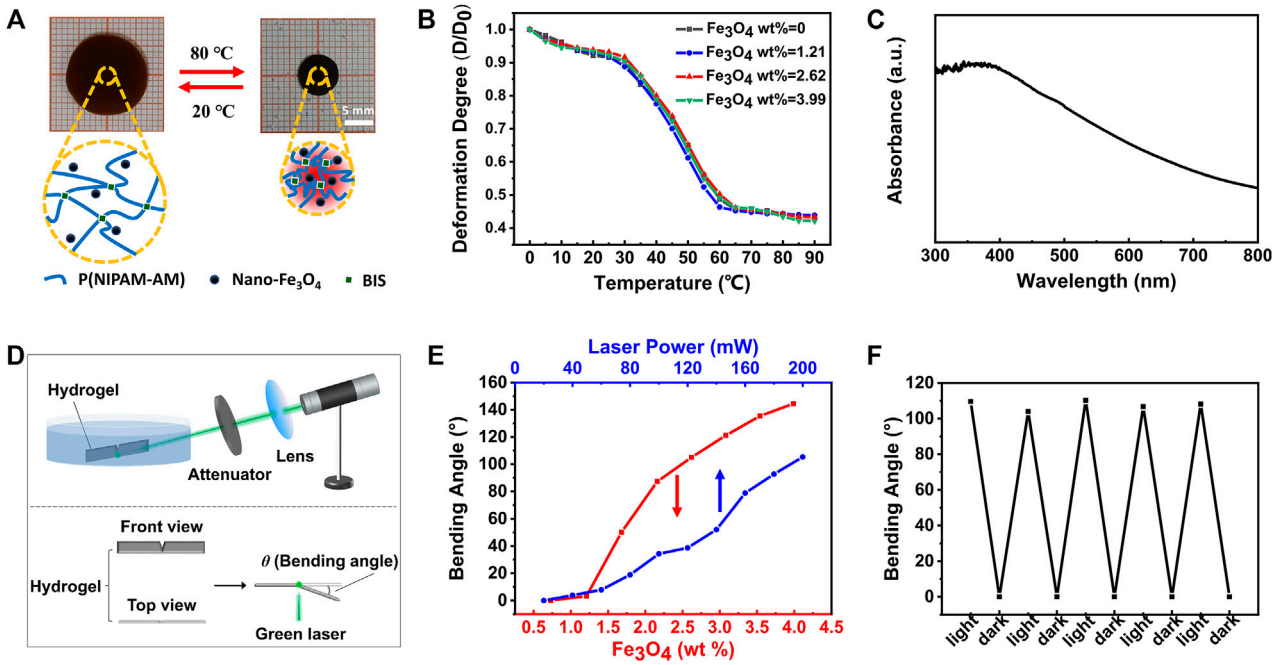

FIGURE 3 | (A) Optical images of P(NIPAM-AM)/Fe_3O_4 hybrid hydrogel with 2.62 wt% Fe_3O_4 NPs in water at 20 and 80°C with the corresponding schematic diagram of deformation mechanism. **(B)** Deformation degree as a function of temperature for hydrogels with different contents of Fe_3O_4 NPs. **(C)** UV–Vis absorbance spectrum of surface-modified Fe_3O_4 NPs/DMSO solution. **(D)** Schematic of the experimental device and 3D hydrogel model for measuring photo-responsive deformation of the hybrid hydrogel. **(E)** Dependences of laser power and contents of Fe_3O_4 NPs on the bending angle of the hydrogel strip. **(F)** Plot of changes in maximum bending angles over five light–dark cycles. Scale bar of **(A)** is 5 mm.

block (weight: 220 mg) was placed near the hydrogel strip. Under an irradiation of a green laser beam (wavelength: 520 nm, power: 200 mW), the temperature of the hydrogel surface at the laser focus ascended from 20 to 58.4°C rapidly (**Figure 4B**). Meanwhile, the hydrogel strip bended with a bending angle up to 59.4°, and the cucumber block was pushed about 47.4 mm. After turning off the laser, the hydrogel strip returned to its original state. It is worth mentioning that cucumber epidermis contains chlorophyll A, which has two strong absorption peaks at 437 and 668 nm (**Figure 4C**). The 520-nm laser used here will give minor damage to the cucumber sample.

Light-Driven Movement

P(NIPAM-AM)/Fe_3O_4 nanocomposite hydrogel can be applied to fabricate visible–light–driven soft actuators for driving a float. Herein, a boomerang-like hydrogel strip (**Supplementary Figure S2**) was fabricated as the driving component to drive floating foam on water (**Figure 5**). The hydrogel strip completely below the water surface (**Figure 5A**) was fixed in the floating foam (**Supplementary Figure S3**). A 520-nm laser was used to irradiate the corner of the hydrogel strip to bring a bending deformation and drive the foam (**Figure 5B**). The incident light moved along the hydrogel strip, and the direction of the incident light and the position of laser focus are relatively fixed with the hydrogel strip.

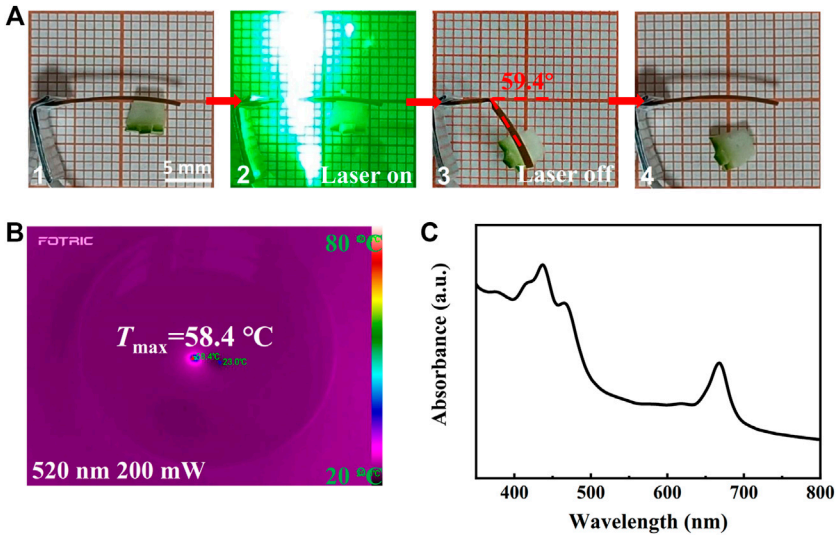

FIGURE 4 | (A) Transportation of the tiny cucumber block by light-driven bending behavior of the hydrogel strip: 1. Vertical view of the strip fixed by a clamp; 2. Laser focused at the hydrogel; 3. Laser was turned off; 4. Hydrogel strip recovered. **(B)** Infrared thermal image of P (NIPAM-AM)/Fe_3O_4 hybrid hydrogel exposed under a green laser (wavelength: 520 nm, power: 200 mW). **(C)** UV–Vis spectrum of chlorophyll-a. Scale bar of **(A)** is 5 mm.

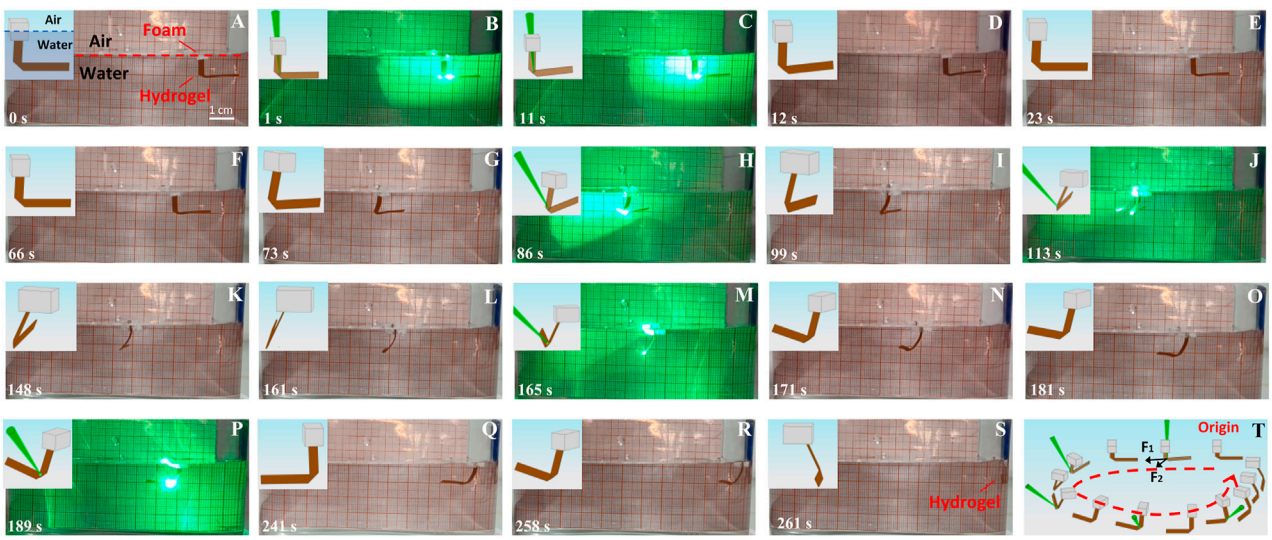

FIGURE 5 | Movement of a float with a boomerang-like hydrogel actuator driven by a 520-nm laser. **(A–S)** Optical images of the floating foam and hydrogel actuator. Inset: three-dimensional (3D) model of the float and hydrogel actuator. **(T)** Moving path of the float and hydrogel actuator. Scale bar of **(A)** is 1 cm.

The laser was turned on for 10 s and off for 13 s as a cycle. It was observed that when the laser was turned on and focused at the middle of the hydrogel, the boomerang-shaped hydrogel actuator obtained an angle-shrinkage deformation, and floating foam was driven to move left (**Figure 5C**). When the laser was turned off, the hydrogel strip gradually recovered from the bending state, which continued to drive the foam left (**Figures 5D,E**). Attributing to the oblique deformation of the hydrogel strip, two forces from water along the tangential (F_1) and normal (F_2) directions of the movement path were induced (**Figure 5T**). Therefore, the path of the float was not a straight line, but an arc. Twelve continuous laser on–off cycles will bring the foam to return to its starting position. Due to the unique design of the boomerang -shaped hydrogel, the whole moving path of the foam on water was near circular (**Figures 5A–T**, **Supplementary Video S1**). The average moving velocities of the foam during laser on and laser off cycles were 0.375 mm s^{-1} and 0.365 mm s^{-1}, respectively.

The key novelty of this study is discussed as follow. First, Fe_3O_4 NPs used here are low cytotoxic materials (Lien et al., 2011) compared with other photothermal conversion agents, such as gold NPs (Ginzburg et al., 2018), graphene oxide (Seabra et al., 2014), and MXene (Huang et al., 2021), which are suitable for biomedical application. Second, light-driven bending deformation of P(NIPAM-AM)/nano-Fe_3O_4 hydrogel in this study is larger than that of PNIPAM/CNTs and PNIPAM/GO hydrogels in literature. Under an irradiation of visible light (0.46 W), the maximum bending angle of PNIPAM/CNTs hydrogel is 80° (Yin et al., 2021). The bending angle of PNIPAM/GO nanocomposite hydrogel under laser irradiation (808 nm, 2.76 W) in water is 32° (Cheng et al., 2019). In this study, the bending angle of the hydrogel strip containing 2.62 wt% Fe_3O_4 under a laser irradiation of 200 mW at 520 nm reaches 107.8°. Third, the traditional strategy for light-driven floating devices is designed basing on Marangoni effect (Wang et al., 2020). Wang et al. prepared asymmetric superhydrophobic polydimethylsiloxane (PDMS) elastomer structures by direct laser writing and controllable visible–light–driven floating devices with fast linear or rotational motions were demonstrated (Wang et al., 2017). In this study, different from previous reports, driving a float by a visible–light–responsive underwater hydrogel actuator is realized. The utilization of hydrogel materials provides the possibility for drug loading. As a prospective study, light-driven hydrogel strip actuators and boomerang-like hydrogel actuators demonstrated in this study have potential applications in tissue repair, drug directional transportation, and vascular cleaning (Zhao et al., 2019).

CONCLUSION

In summary, by incorporating surface-modified Fe_3O_4 NPs, thermal responsive P(NIPAM-AM) hydrogel obtained a good reversible photothermal deformation. It was proven that high Fe_3O_4 content and large laser power induced a large bending deformation of the hybrid hydrogel strip using a 520-nm-laser. For the nanocomposite hydrogel with 2.62 wt% of Fe_3O_4 NPs, the bending angle reached 107.8° with a laser power of 200 mW. A hydrogel strip actuator was applied to transport tiny objects. A boomerang-like hydrogel actuator was designed and fabricated to drive floating foam using a 520-nm-laser. By 12 cycles of laser on–off irradiation upon the hydrogel actuator, a circular returning movement of the float was accomplished with an average moving velocity of ~0.370 mm/s. The green–light–responsive behavior of P (NIPAM-AM)/Fe_3O_4 nanocomposite hydrogel and novel light-driven actuators designed here provide new ideas for the development of visible–light–controlled smart biomedical actuators and soft robots. Attributing to the magnetically responsive property of Fe_3O_4 NPs, the following research is focused on the programmable photomagnetic–field–driven hydrogel actuator, which is underway.

DATA AVAILABILITY STATEMENT

The original contributions presented in the study are included in the article/**Supplementary Material**, further inquiries can be directed to the corresponding authors.

AUTHOR CONTRIBUTIONS

YC carried out the experiment, collected the data, performed the data analyses, and wrote the manuscript. WL contributed to data collection and article writing. FQ revised the manuscript and provided theoretical guidance. YX offered some valuable suggestions on the content of the manuscript. ZX designed and conducted the project. All authors had read and approved the content of the manuscript.

FUNDING

This study was supported by the National Natural Science Foundation of China (61405100); the Natural Science Foundation of Shandong Province (ZR202103050492 and ZR2012EMQ006); and the National College Students Innovative and Entrepreneurial Training Program (No. 202111065288).

SUPPLEMENTARY MATERIAL

The Supplementary Material for this article can be found online at: https://www.frontiersin.org/articles/10.3389/fmats.2022.827608/full#supplementary-material

REFERENCES

Accardo, J. V., McClure, E. R., Mosquera, M. A., and Kalow, J. A. (2020). Using Visible Light to Tune Boronic Acid-Ester Equilibria. *J. Am. Chem. Soc.* 142, 19969–19979. doi:10.1021/jacs.0c08551

Alfredo, A. H., Jorge, L. G., Mercedes, B., Maribel, A. M., Juan, I. S. S, and César, L. C. (2021). Hydrogel-Based Scaffolds in Oral Tissue Engineering. *Front. Mater.* 8, 708945. doi:10.3389/fmats.2021.708945

Chayapol, R., Netipong, B., Marhsilin, K., and Boonsri, K. (2021). Hydrogel Sensors with pH Sensitivity. *Polym. Bull.* 78, 5769–5787. doi:10.1007/s002289-020-03398-8

Chen, J., Huang, J., Zhang, H., and Hu, Y. (2020). A Photoresponsive Hydrogel with Enhanced Photoefficiency and the Decoupled Process of Light Activation and Shape Changing for Precise Geometric Control. *ACS Appl. Mater. Inter.* 12, 38647–38654. doi:10.1021/acsami.0c09475

Cheng, Y., Ren, K., Huang, C., and Wei, J. (2019). Self-healing Graphene Oxide-Based Nanocomposite Hydrogels Serve as Near-Infrared Light-Driven Valves. *Sensors Actuators B: Chem.* 298, 126908. doi:10.1016/j.snb.2019.126908

Fang, G., Yang, X., Wang, Q., Zhang, A., and Tang, B. (2021). Hydrogels-based Ophthalmic Drug Delivery Systems for Treatment of Ocular Diseases. *Mater. Sci. Eng. C* 127, 112212. doi:10.1016/j.msec.2021.112212

Gao, L., Zhang, H., Yu, B., Li, W., Gao, F., Zhang, K., et al. (2020). Chitosan Composite Hydrogels Cross-linked by Multifunctional Diazo Resin as

Antibacterial Dressings for Improved Wound Healing. *J. Biomed. Mater. Res.* 108, 1890–1898. doi:10.1002/jbm.a.36952

Ginzburg, A. L., Truong, L., Tanguay, R. L., and Hutchison, J. E. (2018). Synergistic Toxicity Produced by Mixtures of Biocompatible Gold Nanoparticles and Widely Used Surfactants. *ACS Nano* 12, 5312–5322. doi:10.1021/acsnano.8b00036

Han S, S., Liu, C., Lin, X., Zheng, J., Wu, J., and Liu, C. (2020). Dual Conductive Network Hydrogel for a Highly Conductive, Self-Healing, Anti-freezing, and Non-drying Strain Sensor. *ACS Appl. Polym. Mater.* 2, 996–1005. doi:10.1021/acsapm.9b01198

Han Z, Z., Wang, P., Mao, G., Yin, T., Zhong, D., Yiming, B., et al. (2020). Dual pH-Responsive Hydrogel Actuator for Lipophilic Drug Delivery. *ACS Appl. Mater. Inter.* 12, 12010–12017. doi:10.1021/acsami.9b21713

Huang, M., Gu, Z., Zhang, J., Zhang, D., Zhang, H., Yang, Z., et al. (2021). MXene and Black Phosphorus Based 2D Nanomaterials in Bioimaging and Biosensing: Progress and Perspectives. *J. Mater. Chem. B* 9, 5195–5220. doi:10.1039/d1tb00410g

Jiao, C., Gao, L., Zhang, H., Yu, B., Cong, H., and Shen, Y. (2020). Dynamic Covalent C═C Bond, Cross-Linked, Injectable, and Self-Healable Hydrogels via Knoevenagel Condensation. *Biomacromolecules* 21, 1234–1242. doi:10.1021/acs.biomac.9b01689

Kibungu, C., Kondiah, P. P. D., Kumar, P., and Choonara, Y. E. (2021). This Review Recent Advances in Chitosan and Alginate-Based Hydrogels for Wound Healing Application. *Front. Mater.* 8, 681960. doi:10.3389/fmats.2021.681960

Lee, H. P., Lokhande, G., Singh, K. A., Jaiswal, M. K., Rajput, S., and Gaharwar, A. K. (2021). Light-Triggered *In Situ* Gelation of Hydrogels Using 2D Molybdenum Disulfide (MoS_2) Nanoassemblies as Crosslink Epicenter. *Adv. Mater.* 33, 2101238. doi:10.1002/adma.202101238

Li G, G., Gao, T., Fan, G., Liu, Z., Liu, Z., Jiang, J., et al. (2020). Photoresponsive Shape Memory Hydrogels for Complex Deformation and Solvent-Driven Actuation. *ACS Appl. Mater. Inter.* 12, 6407–6418. doi:10.1021/acsami.9b19380

Li M, M., Wang, X., Dong, B., and Sitti, M. (2020). In-air Fast Response and High Speed Jumping and Rolling of a Light-Driven Hydrogel Actuator. *Nat. Commun.* 11, 3988. doi:10.1038/s41467-020-17775-4

Lien, Y.-H., Wu, T.-M., Wu, J.-H., and Liao, J.-W. (2011). Cytotoxicity and Drug Release Behavior of PNIPAM Grafted on Silica-Coated Iron Oxide Nanoparticles. *J. Nanopart Res.* 13, 5065–5075. doi:10.1007/s11051-011-0487-8

Mantha, S., Pillai, S., Khayambashi, P., Upadhyay, A., Zhang, Y., Tao, O., et al. (2019). Smart Hydrogels in Tissue Engineering and Regenerative Medicine. *Materials* 12, 3323. doi:10.3390/ma12203323

Nawaz, M., Sliman, Y., Ercan, I., Lima-Tenório, M. K., Tenório-Neto, E. T., Kaewsaneha, C., et al. (2019). "Magnetic and pH-Responsive Magnetic Nanocarriers," in *Stimuli Responsive Polymeric Nanocarriers for Drug Delivery Applications*. Editors A. S. H. Makhlouf and A. T. Nedal Y (Duxford: Woodhead Publishing) 2, 37–85. doi:10.1016/B978-0-08-101995-5.00002-7

Pattavarakorn, D., Youngta, P., Jaesrichai, S., Thongbor, S., and Chaimongkol, P. (2013). Electroactive Performances of Conductive Polythiophene/Hydrogel Hybrid Artificial Muscle. *Energ. Proced.* 34, 673–681. doi:10.1016/j.egypro.2013.06.799

Seabra, A. B., Paula, A. J., de Lima, R., Alves, O. L., and Durán, N. (2014). Nanotoxicity of Graphene and Graphene Oxide. *Chem. Res. Toxicol.* 27, 159–168. doi:10.1021/tx400385x

Shang, J., Le, X., Zhang, J., Chen, T., and Theato, P. (2019). Trends in Polymeric Shape Memory Hydrogels and Hydrogel Actuators. *Polym. Chem.* 10, 1036–1055. doi:10.1039/C8PY01286E

Shi, K., Liu, Z., Wei, Y.-Y., Wang, W., Ju, X.-J., Xie, R., et al. (2015). Near-infrared Light-Responsive Poly(*N*-isopropylacrylamide)/Graphene Oxide Nanocomposite Hydrogels with Ultrahigh Tensibility. *ACS Appl. Mater. Inter.* 7, 27289–27298. doi:10.1021/acsami.5b08609

Sun, J., Zhou, F., Hu, H., Li, N., Xia, M., Wang, L., et al. (2020). Photocontrolled Thermosensitive Electrochemiluminescence Hydrogel for Isocarbophos Detection. *Anal. Chem.* 92, 6136–6143. doi:10.1021/acs.analchem.0c00719

Takashima, Y., Hatanaka, S., Otsubo, M., Nakahata, M., Kakuta, T., Hashidzume, A., et al. (2012). Expansion-contraction of Photoresponsive Artificial Muscle Regulated by Host-Guest Interactions. *Nat. Commun.* 3, 1270. doi:10.1038/ncomms2280

Tang, L., Wang, L., Yang, X., Feng, Y., Li, Y., and Feng, W. (2021). Poly(N-isopropylacrylamide)-based Smart Hydrogels: Design, Properties and Applications. *Prog. Mater. Sci.* 115, 100702. doi:10.1016/j.pmatsci.2020.100702

Wang, W., Liu, Y.-Q., Liu, Y., Han, B., Wang, H., Han, D.-D., et al. (2017). Direct Laser Writing of Superhydrophobic PDMS Elastomers for Controllable Manipulation via Marangoni Effect. *Adv. Funct. Mater.* 27, 1702946. doi:10.1002/adfm.201702946

Wang, W., Han, B., Zhang, Y., Li, Q., Zhang, Y. L., Han, D. D., et al. (2020). Laser-Induced Graphene Tapes as Origami and Stick-On Labels for Photothermal Manipulation via Marangoni Effect. *Adv. Funct. Mater.* 31, 2006179. doi:10.1002/adfm.202006179

Xi, H., Zhang, Z., Zhang, W., Li, M., Lian, C., Luo, Q., et al. (2019). All-visible-light-activated Dithienylethenes Induced by Intramolecular Proton Transfer. *J. Am. Chem. Soc.* 141, 18467–18474. doi:10.1021/jacs.9b07357

Xiong, Z., Zheng, C., Jin, F., Wei, R., Zhao, Y., Gao, X., et al. (2018). Magnetic-field-driven Ultra-small 3D Hydrogel Microstructures: Preparation of Gel Photoresist and Two-Photon Polymerization Microfabrication. *Sensors Actuators B: Chem.* 274, 541–550. doi:10.1016/j.snb.2018.08.006

Yang, M., Yuan, Z., Liu, J., Fang, Z., Fang, L., Yu, D., et al. (2019). Photoresponsive Actuators Built from Carbon-Based Soft Materials. *Adv. Opt. Mater.* 7, 1900069. doi:10.1002/adom.201900069

Yin, C., Wei, F., Fu, S., Zhai, Z., Ge, Z., Yao, L., et al. (2021). Visible Light-Driven Jellyfish-like Miniature Swimming Soft Robot. *ACS Appl. Mater. Inter.* 13, 47147–47154. doi:10.1021/acsami.1c13975

Zhao, Y., Xuan, C., Qian, X., Alsaid, Y., Hua, M., Jin, L., et al. (2019). Soft Phototactic Swimmer Based on Self-Sustained Hydrogel Oscillator. *Sci. Robot.* 4, 27. doi:10.1126/scirobotics.aax7112

Zhao, Q., Yu, Z., Liang, Y., Ren, L., and Ren, L. (2021). Intelligent Hydrogel Actuators with Controllable Deformations and Movements. *Front. Mater.* 8, 661104. doi:10.3389/fmats.2021.661104

Zheng, C., Jin, F., Zhao, Y., Zheng, M., Liu, J., Dong, X., et al. (2020). Light-driven Micron-Scale 3D Hydrogel Actuator Produced by Two-Photon Polymerization Microfabrication. *Sensors Actuators B: Chem.* 304, 127345. doi:10.1016/j.snb.2019.127345

Zhou, S., Zhou, Q., Wang, M., Zhang, Z., and Ren, L. (2020). Preparation of Bilayer Shape Memory Intelligent Hydrogel Actuators and Their Structural Characteristics. *Int. J. Food Properties* 23, 470–480. doi:10.1080/10942912.2020.1733601

Conflict of Interest: The authors declare that the research was conducted in the absence of any commercial or financial relationships that could be construed as a potential conflict of interest.

Publisher's Note: All claims expressed in this article are solely those of the authors and do not necessarily represent those of their affiliated organizations, or those of the publisher, the editors, and the reviewers. Any product that may be evaluated in this article, or claim that may be made by its manufacturer, is not guaranteed or endorsed by the publisher.